

Exploration of the mechanism for LPFFD inhibiting the formation of β -sheet conformation of $A\beta(1-42)$ in water

Cao Yang · Xiaolei Zhu · Jinyu Li · Rongwei Shi

Received: 28 July 2009 / Accepted: 11 September 2009 / Published online: 5 January 2010
© Springer-Verlag 2009

Abstract The main component of senile plaques found in AD brain is amyloid β -peptide ($A\beta$), and the neurotoxicity and aggregation of $A\beta$ are associated with the formation of β -sheet structure. Experimentally, beta sheet breaker (BSB) peptide fragment Leu-Pro-Phe-Phe-Asp (LPFFD) can combine with $A\beta$, which can inhibit the aggregation of $A\beta$. In order to explore why LPFFD can inhibit the formation of β -sheet conformation of $A\beta$ at atomic level, first, molecular docking is performed to obtain the binding sites of LPFFD on the $A\beta(1-42)$ (LPFFD/ $A\beta(1-42)$), which is taken as the initial conformation for MD simulations. Then, MD simulations on LPFFD/ $A\beta(1-42)$ in water are carried out. The results demonstrate that LPFFD can inhibit the conformational transition from α -helix to β -sheet structure for the C-terminus of $A\beta(1-42)$, which may be attributed to the hydrophobicity decreasing of C-terminus residues of $A\beta(1-42)$ and formation probability decreasing of the salt bridge Asp23-Lys28 in the presence of LPFFD.

Keywords $A\beta(1-42)$ · Conformational transition · LPFFD · Molecular docking · Molecular dynamics simulation

Introduction

Alzheimer's disease (AD) is characterized by conformational changes and aggregation of amyloid β -peptide ($A\beta$) in brains. $A\beta$ is a proteolytic product of larger amyloid precursor protein (APP) and consists of 39–43 residues [1].

The deposits of $A\beta$ with the form of amyloid fibrils are widespread in senile plaques and in cerebral and meningeal blood vessels [2, 3]. Although many other forms of $A\beta$, such as $A\beta(1-40)$, are also present in cerebrovascular amyloid deposits, the 42-amino acid form of $A\beta$ ($A\beta(1-42)$) is found to be the predominant species of $A\beta$ in both diffuse and senile plaques within the AD brain [4–6]. Accumulating evidence shows that $A\beta(1-42)$ undergoes spontaneous rearrangement of its initial secondary structure, generating oligomeric and polymeric species with higher content of β -sheet structure, and such structural transition can be inhibited by many factors [7–12].

The secondary structure determines several importance properties of $A\beta$ that may be relevant to the pathogenesis of AD. Firstly, the neurotoxicity of amyloid peptide is associated with formation of β -sheet structure [13–19] or amyloid fibrils [20]. Secondly, the ability of $A\beta$ to form amyloid fibrils is directly related to the content of β -sheet structure adopted by the peptides [21], and it has been proposed that peptides with high content of β -sheet structure can act as seeds for nucleation and fibrils formation [22, 23]. Finally, $A\beta$ with high content of β -sheet is more resistant to proteolytic degradation of amyloid deposits and associated with the disease process [24]. Therefore, one can reduce the neurotoxicity and inhibit the aggregation of $A\beta$ by preventing the formation of β -sheet structure in $A\beta$.

Some non-peptide inhibitors and peptide inhibitors are designed to prevent the formation of β -sheet structure and amyloid aggregation [25–33]. These are so-called beta sheet breakers (BSBs) and considered to be potential AD drugs. Most non-peptide inhibitors are organic compounds, which are found to inhibit or reduce the aggregation and toxicity of $A\beta$ in vitro. These compounds include nicotine [25, 26], hexadecyl-N-methylpip- eridium bromide [27],

C. Yang · X. Zhu (✉) · J. Li · R. Shi
State Key Laboratory of Materials-Oriented Chemical
Engineering, College of Chemistry and Chemical Engineering,
Nanjing University of Technology,
Nanjing 210009, China
e-mail: xlzhu@njut.edu.cn

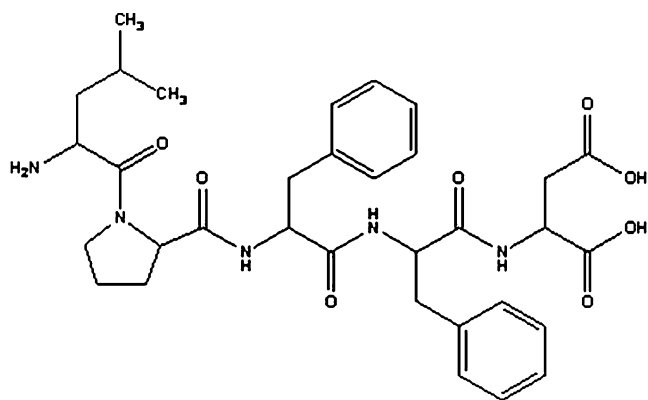
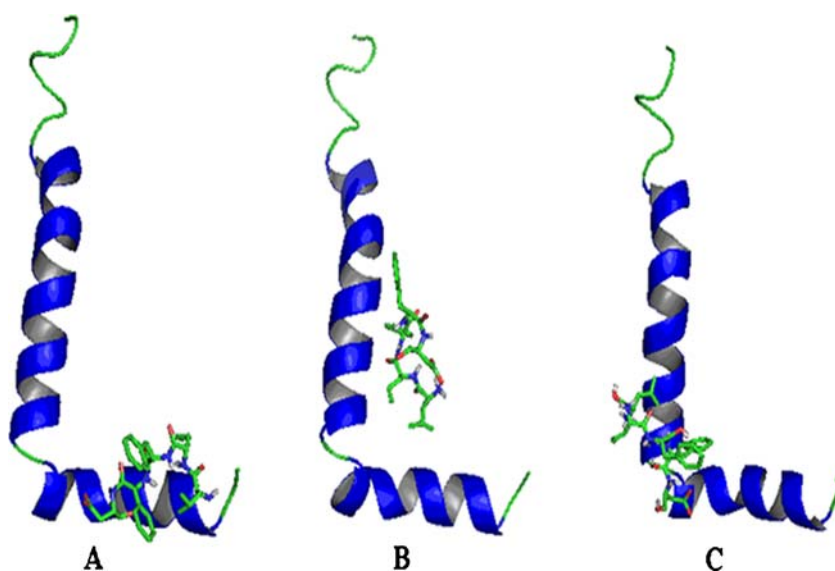


Fig. 1 The chemical structure of LPFFD

anthracycline 4'-iodo-4'-deoxydoxorubicin [28], amphiphilic surfactants [29], and so on. However, peptide inhibitors are more attractive to inhibit the aggregation of A β because they are peptide fragments derived from A β and can recognize other A β s during aggregation. Tjernberg et al. [30] first discovered that the small peptide Lys-Leu-Val-Phe-Phe (KLVFF) is able to combine with full-length A β and prevent its assembly into fibrils. By modification of this pentapeptide, Soto et al. [31] designed a similar peptide with an aromatic core: Leu-Pro-Phe-Phe-Asp (LPFFD), which can act as BSB. In the presence of this molecule, the amyloid fibrils can be disassembled [32]. One of their strategies is to substitute key residues in order to reduce the β -sheet propensity, which is very important for designing AD drugs. Some research groups have followed this strategy to design different kinds of peptide inhibitors and studied their effect on the A β aggregation [33]. However, it remains unclear why they can inhibit the formation of β -sheet conformation of A β at atomic level.

Fig. 2 The structures of three complexes (A β (1–42)/LPFFD) obtained from docking calculations. The number of conformations in each cluster and their average docking energies are as follows: **a**: 66, $-25.2 \text{ kJ mol}^{-1}$; **b**: 59, $-17.7 \text{ kJ mol}^{-1}$; **c**: 48, $-14.9 \text{ kJ mol}^{-1}$



The first attempt to elucidate the binding site of BSB peptides on the A β molecule is made with the aid molecular docking by Hetenyi et al. [34]. They selected four BSB peptides and employed molecular docking to find out their binding sites on the A β (6–34) and their intermolecular interaction energies. However, there are few reports about the mechanism of these BSB peptides inhibiting the formation of β -sheet structure in the C-terminus of A β (1–42). In current work, we identify the binding sites of LPFFD on the full length A β (1–42) via molecular docking and explore how LPFFD inhibit the β -sheet formation of C-terminus of A β (1–42) in water using MD simulation techniques, which is helpful for designing new AD drugs.

Computational methods

The structure of A β (1–42) used in the docking calculations is obtained from the Protein Data Bank (1IYT) [35]. The structure of β -sheet breaker (BSB) peptide LPFFD is shown in Fig. 1. For ligand, random starting position, orientation, and torsion are used in order to search flexible conformations of the compounds during the docking process. Program Autodock 4 [36] is applied to carry out the automated molecular docking with Lamarckian genetic algorithm. The grid map with $80 \times 80 \times 80$ points spaced equally at 0.375 \AA is generated using AutoGrid program to evaluate the binding energies between the ligand and receptor. Docking parameters are set to default values except for the number of GA runs (200) and the energy evaluations (25000000). At the end of the run, all docked conformations are clustered using a tolerance of 2 \AA for

root mean square deviation (RMSD) and ranked based on docking energies.

We select the complex A (see Fig. 2) as the initial structure of LPFFD/A β (1–42) in MD simulations. MD simulations are performed applying GROMACS 3.3.3 MD package [37, 38] with the GROMOS96 43A1 force field [39]. The united atom topology file for LPFFD is generated using the PRODRG server [40]. The complex is placed in a cubic simulation box of dimensions 73.186 Å \times 73.186 Å \times 73.186 Å, and the minimal distance from the complex to the edge of box is 1.0 nm. Then, the system is solvated with water molecules, neutralized with counterions, and the single point charge (SPC) model for water is used in the simulations. All bond lengths are constrained using the LINCS algorithm with a time steps of 2 fs [41]. The system is first minimized using steepest descent algorithms for 2000 steps to avoid unreasonable contacts. Then, we perform 30 ns MD simulations for the system with the NPT ensemble. The pressure is coupled to 1 bar with an anisotropic coupling time of 1.0 ps and the temperature is kept at 300 K during the simulations with a coupling time of 0.1 ps. Both pressure and temperature are controlled using Berendsen coupling protocols [42]. The long-range electrostatic interactions are calculated by the particle-mesh ewald (PME) method [43, 44]. Two cut-offs of 0.8 and 1.4 nm are used for the evaluation of the non-bonded interactions.

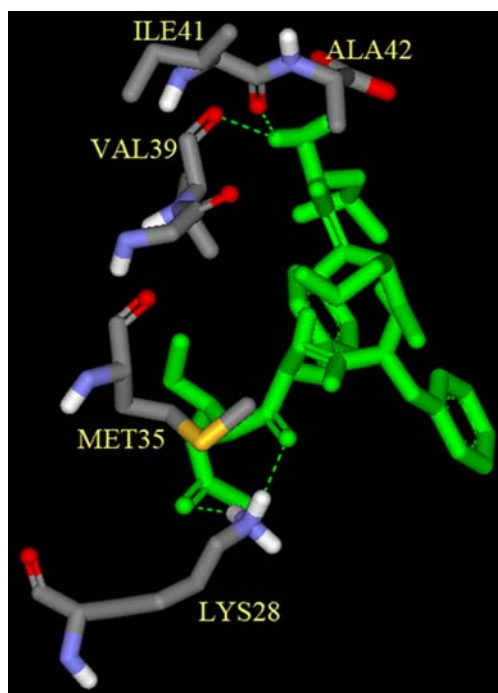


Fig. 3 Associate of LPFFD and the C-terminus of A β (1–42) obtained from docking calculations. There are four hydrogen bonds (dashed line) between LPFFD and residues of A β (1–42) under the condition of vacuum

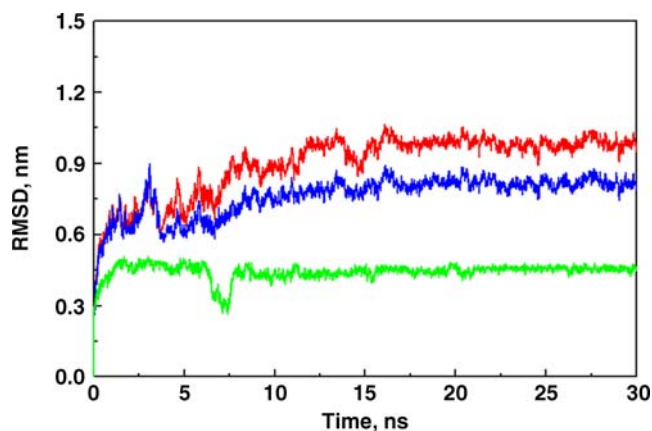


Fig. 4 RMSDs of LPFFD (green), A β (1–42) (blue), and the complex (red) compared to their original conformations as a function of time

Analysis of the MD simulations is made using the various GROMACS tools. The secondary structure of A β (1–42) in the complex is characterized by DSSP [45]. The 3D figures are plotted using the software of VMD [46].

Results and discussion

Our previous work [47] demonstrates that most residues in the C-terminus of A β (1–42) adopt β -sheet structure in water, and the formation of β -sheet structure may promote the aggregation of A β (1–42). As mentioned above, some small molecules combined with the C-terminus of A β (1–42) would inhibit the conformation transition from initial α -helix to β -sheet. In order to explore the reason why LPFFD can inhibit conformation transition of C-terminus of A β (1–42) in water, we carry out the docking calculations and MD simulations on A β (1–42)/LPFFD.

According to the docking energies and cluster tolerance, the docked conformations are divided into three main

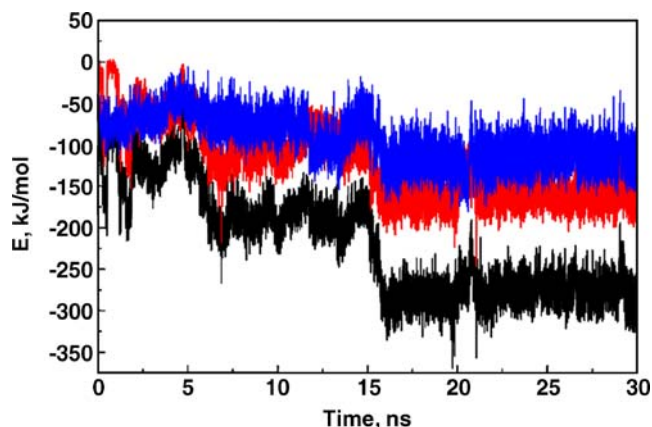
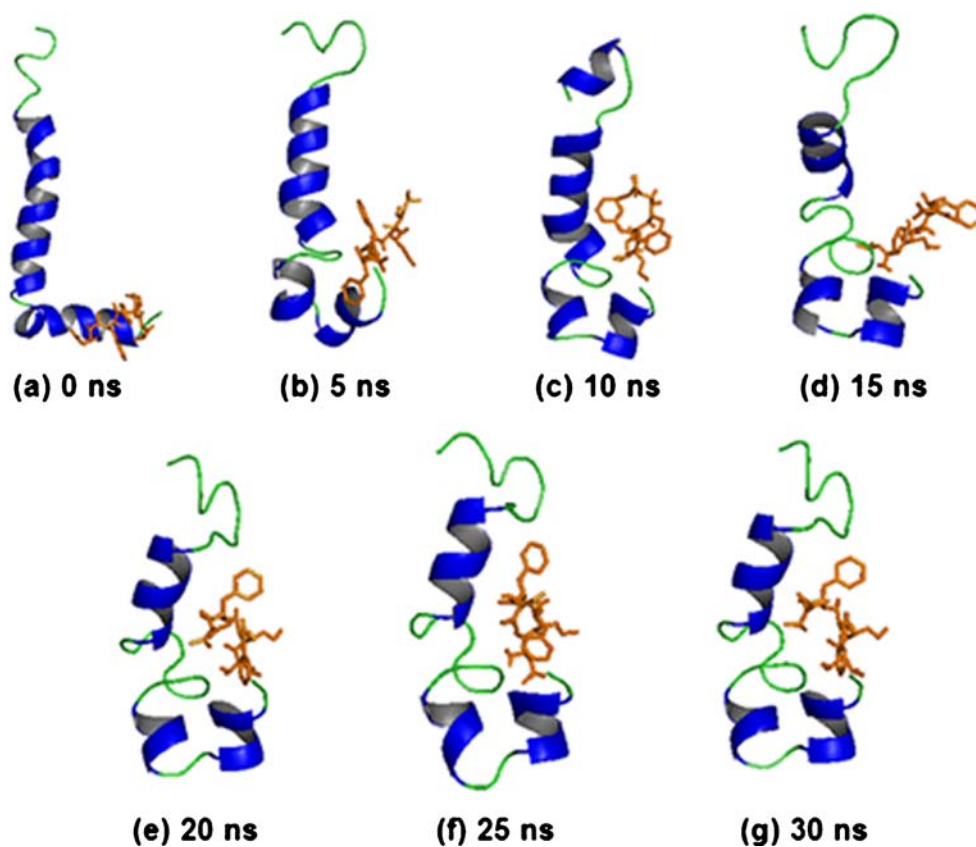


Fig. 5 The electrostatic energy (red), Van der Waals energy (blue) and total interaction energy (black) between LPFFD and A β (1–42) with time evolution

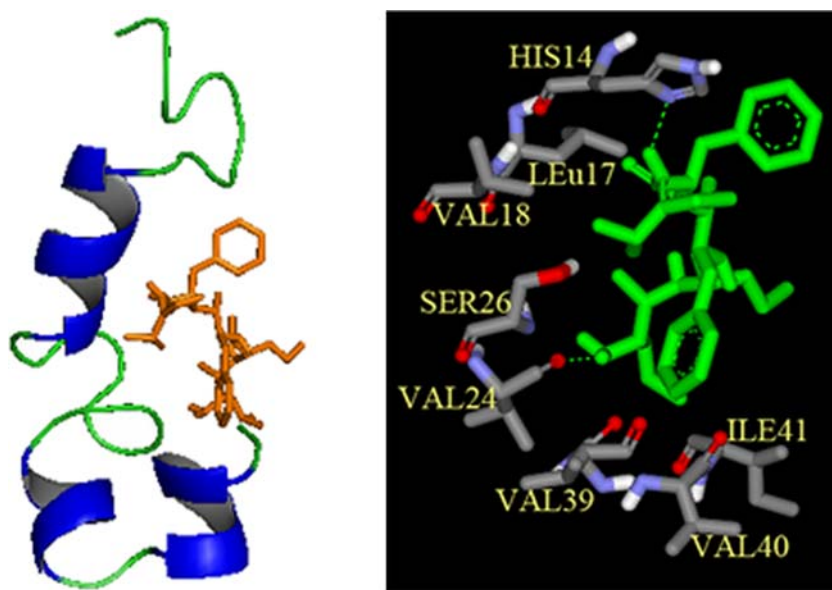
Fig. 6 The snapshots of the simulations at every 5 ns interval



clusters and the complex structures of the three clusters are shown in Fig. 2. The number of conformations in each cluster and their average docking energies are as follows: complex A: 66, $-25.2 \text{ kJ mol}^{-1}$; complex B: 59, $-17.7 \text{ kJ mol}^{-1}$; complex C: 48, $-14.9 \text{ kJ mol}^{-1}$. It is not difficult to see from Fig. 2 that LPFFD locates at the C-terminal of

$\text{A}\beta(1-42)$ for complex A, and the detailed docking information of the complex A is shown in Fig. 3. There are four hydrogen bonds between LPFFD and residues of the C-terminus of $\text{A}\beta(1-42)$ in vacuum, which may be favorable to stabilizing the initial α -helix structure in the C-terminus of $\text{A}\beta(1-42)$. Therefore, we select this complex A

Fig. 7 The structure of complex (left) and detailed binding mode of the complex (right) after 30 ns MD simulations



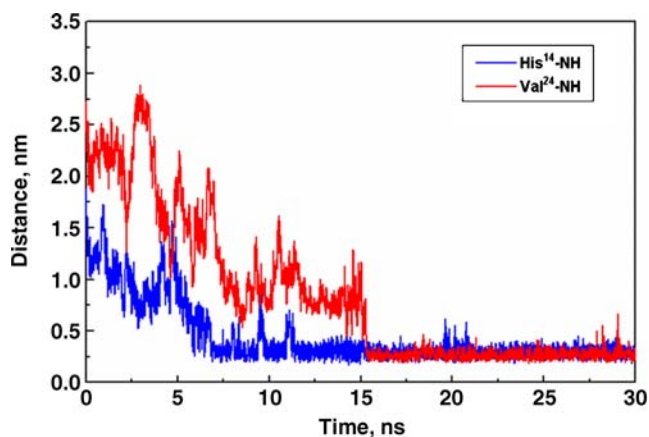


Fig. 8 The hydrogen-bond distance between A β (1–42) and LPFFD with time evolution

as the starting conformation of MD simulations and investigate the effect of LPFFD on the conformation of A β (1–42) in the water.

In order to examine the stability of the complex in the water during MD simulations, the root mean square distances (RMSDs) are calculated and shown in Fig. 4. Clearly, it can be seen from Fig. 4 although A β (1–42) exhibits conformational change, the RMSDs of LPFFD, A β (1–42), and A β (1–42)/LPFFD stay constant after 16 ns. The total interaction energies between LPFFD and A β (1–42) are plotted against the simulation time as shown in Fig. 5. It is not difficult to see from Fig. 5 that the total interaction energies significantly drop near 5 ns and 15 ns and stay constant after 16 ns, which is in agreement with the RMSD results. It suggests that the complex obtained from MD simulations is relatively stable.

In docking calculations under vacuum condition, we obtain the relatively better complex structure (complex A) with LPFFD locating around the C-terminus of A β (1–42) as shown in Fig. 2. During MD simulations of complex A in water, the presence of water will result in the conformational change of the complex. Figure 6 represents

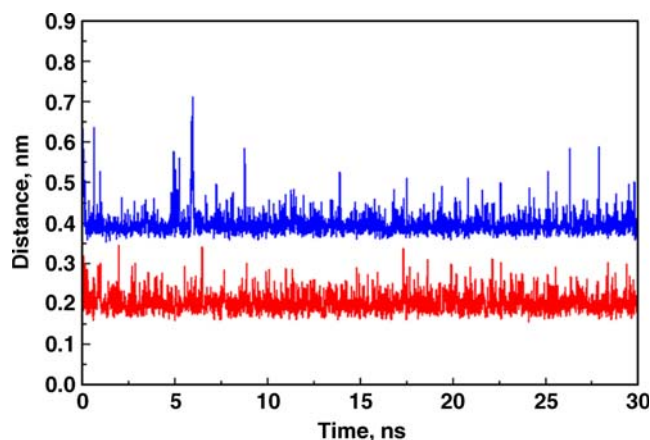


Fig. 10 The time dependence of distance between carboxyl oxygen and amide hydrogen for Lys28-Val32 (red) and Met35-Val40 (blue). To enhance the visual clarity, the curve of Met35-Val40 is shifted upward by 0.2 nm

the snapshots of the simulations at every 5 ns intervals. It should be noted from Fig. 6 that the binding mode between LPFFD and A β (1–42) continually changes before 15 ns and approximately keeps constant after 15 ns, which is consistent with the results from Fig. 5. The final structure of the complex after 30 ns MD simulations is shown in Fig. 7. Comparing with the initial complex structure (Fig. 6 (a)), the C-terminus of A β (1–42) in equilibrium structure of the complex exhibits bent upward, and the small molecule LPFFD moves to the middle region of A β (1–42) (Fig. 6 (g)). As is shown in Fig. 7, there are two hydrogen bonds between A β (1–42) and LPFFD. The time dependence of distances for these two hydrogen bonds are shown in Fig. 8. It can be seen from Fig. 8 that there are two hydrogen bonds with averaged 0.25 nm between LPFFD and A β (1–42), which play an important role in the stability of the complex (LPFFD /A β (1–42)).

The time dependence of secondary structure for A β (1–42) in the complex is shown in Fig. 9. The content of α -helix structure gradually decreases in the N-

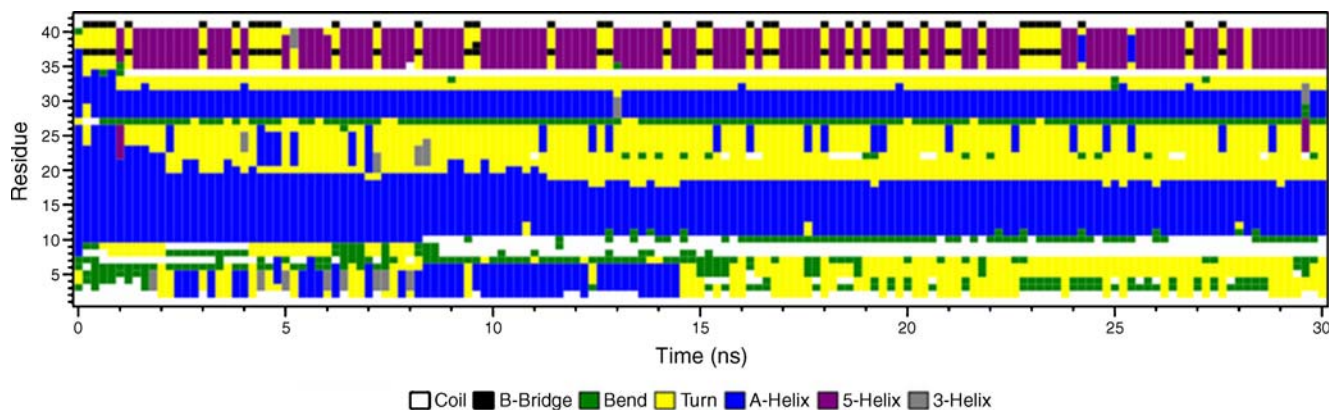


Fig. 9 The time evolution of the secondary structure of A β (1–42) in presence of LPFFD

terminus of A β (1–42), but the residues 10–18 adopt α -helix structure throughout the simulations. In the C-terminus of A β (1–42), the α -helix and turn structure of residues 35–40 converts into 5-helix structure after 1 ns and this region mainly adopts 5-helix structure, with occasionally converting into turn structure and recovering to 5-helix structure rapidly. The C-terminus residues 28–32 adopt α -helix structure during the simulations. The remaining residues in C-terminus of A β (1–42) adopt turn structure, no β -sheet structure is observed. The results indicate that the secondary structure of A β (1–42) with LPFFD binding in water is significantly different from that of A β (1–42) in water [47]. Experimental and calculated results [47–51] demonstrate that the C-terminus of A β (1–42) in water adopts β -sheet structure. However, for LPFFD /A β (1–42) in water, most residues of the C-terminus of A β (1–42) adopt helix structure, which may be related to the presence of LPFFD.

As mentioned above, LPFFD is located in the middle region of A β (1–42) after 16 ns and forms hydrogen bonds with the middle residues, the position of LPFFD is similar to that of LPFFD in the docking complex structure B (see Fig. 2). In fact, we also perform MD simulations to investigate the conformational behavior of complex structure B in water. It is surprising to note that the initial helix structure in the C-terminus of A β (1–42) is changed into β -sheet structure. It reveals that the LPFFD plays a delicate role in the stabilizing of the C-terminal helix structure of A β (1–42) for complex A in water.

To further illustrate the stability of helix structure in the C-terminus of A β (1–42) for complex A in water, we calculate the distance between carbonyl oxygen and amide hydrogen for two pairs of residues: Lys28-Val32 and Met35-Val40. The time evolution of oxygen-hydrogen distance for these two pairs of residues is shown in Fig. 10. The distance between carbonyl oxygen

of Lys28 and amide hydrogen of Val32 stays around 0.25 nm during the simulations, which suggests that a hydrogen bond forms between Lys28 and Val32 and is favorable to stabilize α -helix conformation from Lys28 to Val32, which is consistent with the result from the analysis of secondary structure. Although the distance between carbonyl oxygen of Met35 and amide hydrogen of Val40 is occasionally larger than 0.35 nm during MD simulations, the distance also stays around 0.25 nm within most simulation time.

It is widely accepted that the formation of the salt bridge between Asp23 and Lys28 in the monomer folding plays a vital role in the aggregation of A β [52–54]. Experimental study also showed that Asp23 and Lys28 form a salt bridge in A β (1–42) fibrils [55]. It is defined that the salt bridge forms when the distance between C $^{\gamma}$ of Asp23 and the N $^{\zeta}$ of Lys28 is less than 0.5 nm. We record structure every 1 ps in the simulations and obtain 3×10^4 structures. For A β (1–42) and A β (1–42)/LPFFD in water, 41% and 10% of the structures form the Asp23-Lys28 salt bridge structures, respectively. Moreover, the distance distributions between the Asp23 and Lys28 for the A β (1–42) and LPFFD /A β (1–42) are

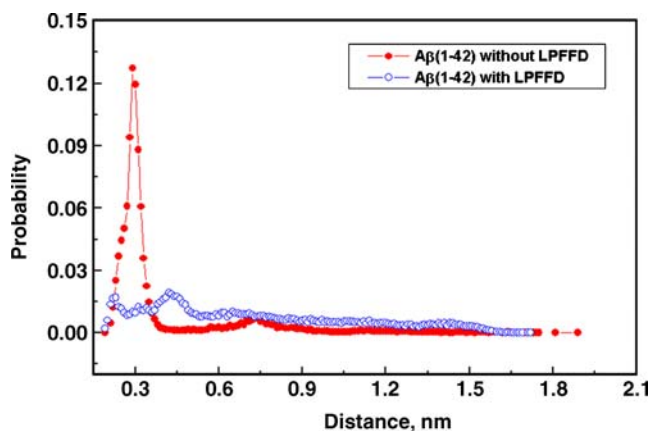


Fig. 11 Distance distributions between the Asp23 and Lys28 for the A β (1–42) with (solid circle) and without LPFFD binding (open circle) in water at 300 K

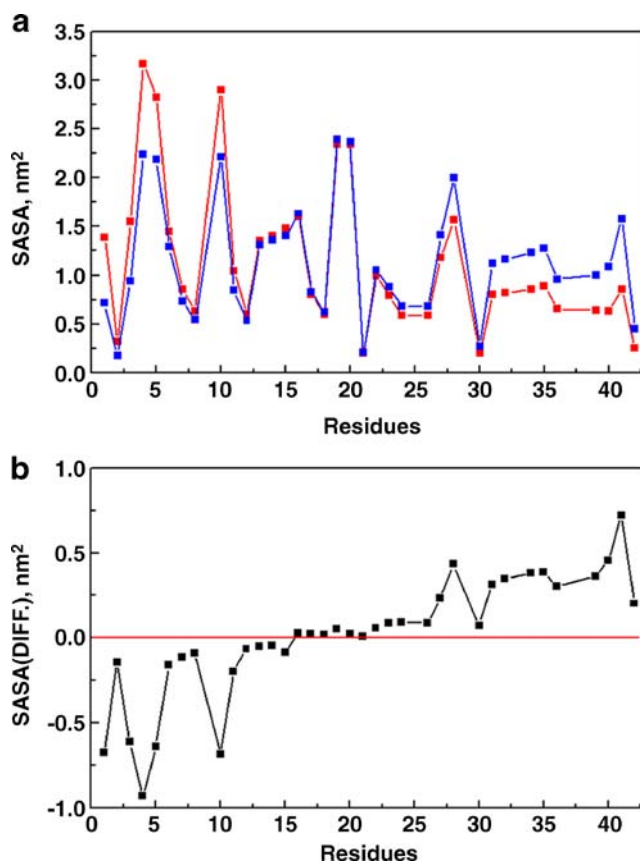


Fig. 12 (a) SASA for the side-chain atoms of A β (1–42) with (blue) and without (red) LPFFD binding in water; (b) Difference in SASA values for A β (1–42) with and without LPFFD binding

shown in Fig. 11. At the distance around 0.3 nm, there exists a sharp peak for the distance distributions between Asp23 and Lys28 in the A β (1–42) without LPFFD binding, which reveals the formation of Asp23–Lys28 salt bridge. However, there are only two small peaks in the case of LPFFD/A β (1–42), that is, A β (1–42)/LPFFD has a lower formation probability of the Asp23–Lys28 salt bridge than A β (1–42). As shown in Fig. 5, the electrostatic interaction between A β (1–42) and LPFFD has a significant contribution to the total energy of the complex. The competition between intermolecular electrostatic interaction and the intrapeptide electrostatic interaction leads to the disruption of Asp23–Lys28 salt bridge. On the other hand, the formation of hydrogen bonds between LPFFD and A β (1–42) may not be favorable to the formation of the Asp23–Lys28 salt bridge in the monomer.

It was proposed that the helix structure correlates with the hydrophilicity of residues and β -sheet structure is stabilized by the hydrophobic interactions [56]. Thus, we compute the solvent accessible surface area (SASA) per residue to assess the extent of hydrophobic burial of different regions in the A β (1–42) with and without LPFFD binding (Fig. 12(a)). The differences in SASA values per residue between LPFFD/A β (1–42) and A β (1–42) are shown in Fig. 12(b). The positive and negative values in Fig. 12(b) reflect the decreasing and increasing in the hydrophobic character of residues, respectively. It is not difficult to see from Fig. 12(b) that the hydrophobicity of C-terminal residues in A β (1–42) decreases in presence of LPFFD, which are favorable to the stability of helix structures in the C-terminus of A β (1–42). In addition, the increases of hydrophobicity for N-terminal residues of A β (1–42) with LPFFD binding lead to the loss of some α -helix structures as shown in Fig. 9.

Conclusions

In summary, we use molecular docking and MD simulation techniques to explore the mechanisms for LPFFD inhibiting the conformational transition of C-terminus in A β (1–42) from α -helix to β -sheet structure. Our MD simulations on LPFFD/A β (1–42) reveal several important results: (i) there are hydrogen bonds between LPFFD and A β (1–42), which is one important factor for stabilizing complex (LPFFD/A β (1–42)); (ii) the presence of LPFFD inhibits the conformational transition of C-terminus in A β (1–42) from α -helix to β -sheet structure, which is in agreement with the available experimental results; (iii) the presence of LPFFD inhibits the formation of Asp23–Lys28 salt bridge and decreases the hydrophilicity of C-terminus residues of

A β (1–42), which is one of the possible mechanisms for LPFFD preventing the conformational transition of A β (1–42) from α -helix to β -sheet structure in water and aggregation of the A β (1–42). Our current work will be helpful for the design of new BSBs that will inhibit the β -sheet of A β (1–42) more effectively.

Acknowledgments This work is supported by grants from the National Science Foundation of China (No. 20706029, 20876073), Jiangsu Science and Technology Department of China (BK2008372), and Nanjing University of Technology of China (No. ZK200803).

References

- Kang J, Lemaire HG, Unterbeck A, Salbaum JM, Masters CL, Grzeschik KH, Multhaup G, Beyreuther K, Muller-Hill B (1987) The precursor of Alzheimer's disease amyloid A4 protein resembles a cell-surface receptor. *Nature* 325:733–736
- Chromy BA, Nowak RJ, Lambert MP, Viola KL, Chang L, Velasco PT, Jones BW, Fernandez SJ, Laco'r PN, Horowitz P, Finch CE, Krafft GA, Klein WL (2003) Self-assembly of A β into globular neurotoxins. *Biochemistry* 42:12749–12760
- Hardy JA, Higgins GA (1992) Alzheimer's disease: the amyloid cascade hypothesis. *Science* 256:184–185
- Iwatsubo T, Odaka A, Suzuki N, Mizusawa H, Nukina N, Ihara Y (1994) Visualization of A β 42(43) and A β 40 in senile plaques with end-specific A β monoclonals: evidence that an initially deposited species is A β 42(43). *Neuron* 13:45–53
- Gravina SA, Ho L, Eckman CB, Long KE, Otvos L, Younkin LH, Suzuki N, Younkin SG (1995) Amyloid β protein (A β) in Alzheimer's disease brain. *J Biol Chem* 270:7013–7016
- Golde TE, Eckman CB, Younkin SG (2000) Biochemical treatment of Alzheimer's disease. *Biochim Biophys Acta* 1502:172–187
- Barrow CJ, Zagorski MG (1991) Solution structure of β peptide and its constituent fragments: relation to amyloid deposition. *Science* 253:179–181
- Barrow CJ, Yasuda A, Kenny PTM, Zagorski MG (1992) Solution conformations and aggregational properties of synthetic amyloid β -peptides of Alzheimer's disease. *J Mol Biol* 225:1075–1093
- Hilbich C, Kisters-Woide B, Reed J, Masters CL, Beyreuther K (1991) Aggregation and secondary structure of synthetic amyloid β A4 peptides of Alzheimer's disease. *J Mol Biol* 218:149–163
- Kirchner DA, Inouye H, Duffy LK, Sinclair A, Lind M, Selkoe D (1987) Synthetic peptide homologous to beta protein from Alzheimer disease forms amyloid-like fibrils in vitro. *Proc Natl Acad Sci USA* 84:6953–6957
- Gorevic PD, Castano EM, Sarma R, Frangione B (1987) Ten to fourteen residue peptides of Alzheimer's disease protein are sufficient for amyloid fibril formation and its characteristic x-ray diffraction pattern. *Biochem Biophys Res Commun* 147:854–862
- Shen CL, Murphy RM (1995) Solvent effects on self-assembly of β -amyloid peptide. *Biophys J* 69:640–651
- Behl C, Davis JB, Lesley R, Schubert D (1994) Hydrogen peroxide mediates amyloid β protein toxicity. *Cell* 77:817–827
- Harris ME, Hensley K, Butterfield DA, Leedle RA, Carney JM (1995) Direct evidence of oxidative injury produced by the Alzheimer's β -amyloid peptide (1–40) in culture hippocampal neurons. *Exp Neurol* 131:193–202
- Buchet R, Tavittian E, Ristig D, Swoboda R, Stauss U, Gremlich HU, Fourniere LL, Staufenbiel M, Frey P, Lowe DA (1996) Conformations of synthetic β peptides in solid state and in

- aqueous solution: relation to toxicity in PC12 cells. *Biochim Biophys Acta* 1315:40–46
16. Simmons LK, May PC, Tomaselli KJ, Rydel RE, Fuson KS, Brigham EF, Wright S, Lieberburg I, Becker GW, Brems DN (1994) Secondary structure of amyloid beta peptide correlates with neurotoxic activity in vitro. *Mol Pharmacol* 45:373–379
 17. Greenfield NJ, Fasman GD (1969) Computed circular dichroism spectra for the evaluation of protein conformation. *Biochemistry* 8:4108–4116
 18. Tomski S, Murphy RM (1992) Kinetics of aggregation of synthetic β -amyloid peptide. *Arch Biochem Biophys* 294:630–638
 19. Walencewicz-Wasserman AJ, Kosmoski J, Cribbs DH, Glabe CG, Cotman CW (1995) Structure-activity analyses of β -peptides: conformations of the β 25–35 region to aggregation and neurotoxicity. *J Neurochem* 64:253–265
 20. Lorenzo A, Yankner BA (1994) Beta-amyloid neurotoxicity requires fibril formation and is inhibited by congo red. *Proc Natl Acad Sci USA* 91:12243–12447
 21. Soto C, Castano EM, Kumar RA, Beavis R, Frangione CB (1995) Fibrillogenesis of synthetic amyloid- β peptides is dependent on their initial secondary structure. *Neurosci Lett* 200:105–108
 22. Jarrett JT, Berger EP Jr, Lansbury PT (1993) The carboxy terminus of the β amyloid protein is critical for the seeding of amyloid formation: implications for the pathogenesis of Alzheimer's disease. *Biochemistry* 32:4693–4697
 23. Snyder SW, Lador US, Wade WS, Wang GT, Barrett LW, Matayoshi ED (1994) Amyloid- β aggregation: selective inhibition of aggregation in mixtures of amyloid with different chain lengths. *Biophys J* 67:1216–1228
 24. Soto C, Castano EM (1996) The conformation of Alzheimer's β peptide determines the rate of amyloid formation and its resistance to proteolysis. *Biochem J* 314:701–707
 25. Salomon AR, Marcinowski KJ, Friedland RP, Zagorski MG (1996) Nicotine inhibits amyloid formation by the β -peptide. *Biochemistry* 35:13568–13578
 26. Moore SA, Huckerby TN, Gibson GL, Fullwood NJ, Turnbull S, Tabner BJ, El-Agnaf OM, Allsop D (2004) Both the D-(+) and L-(-) enantiomers of nicotine inhibit A β aggregation and cytotoxicity. *Biochemistry* 43:819–826
 27. Wood SJ, MacKenzie L, Maleef B, Hurle MR, Wetzel R (1996) Selective inhibition of A β fibril formation. *J Biol Chem* 271:4086–4092
 28. Merlini G, Ascari E, Amboldi N, Bellotti V, Arbustini E, Perfetti V, Ferrari M, Zorzoli I, Marinone MG, Garini P, Diegoli M (1995) Interaction of the anthracycline 4'-iodo-4'-deoxydoxorubicin with amyloid fibrils: inhibition of amyloidogenesis. *Proc Natl Acad Sci USA* 92:2959–2963
 29. Wang SS, Chen YT, Chou SW (2005) Inhibition of amyloid fibril formation of β -amyloid peptides via the amphiphilic surfactants. *Biochim Biophys Acta* 1741:307–313
 30. Tjernberg LO, Näslund J, Lindqvist F, Johansson J, Karlström AR, Thyberg J, Terenius L, Nordstedt C (1996) Arrest of β -amyloid fibril formation by a pentapeptide ligand. *J Biol Chem* 271:8545–8548
 31. Soto C, Sogurdsson EM, Morello L, Kumar RA, Castano EM, Frangione B (1998) B-sheet breaker peptides inhibit fibrillogenesis in a rat brain model of amyloidosis: implications for Alzheimer's therapy. *Nat Med* 4:822–826
 32. Soto C, Saborio GP, Permann B (2000) Inhibit the conversion of soluble amyloid-beta peptide into abnormally folded amyloidogenic intermediates: relevance for Alzheimer's disease therapy. *Acta Neurol Scand Suppl* 176:90–95
 33. Andrew JD (2007) Peptide inhibitors of β -amyloid aggregation. *Curr Opin Drug Discov Devel* 10:533–539
 34. Hetényi C, Kortvelyesi T, Penke B (2001) Computational studies on the binding of β -sheet breaker (BSB) peptides on amyloid β A (1–42). *THEOCHEM* 542:25–31
 35. Crescenzi O, Tomaselli S, Guerrini R, Salvadori S, D'Ursi AM, Temussi PA, Picone D (2002) Solution structure of the Alzheimer amyloid β -peptide (1–42) in an apolar microenvironment. *Eur J Biochem* 269:5642–5648
 36. Morris GM, Goodsell DS, Halliday RS, Huey R, Hart WE, Belew RK, Olson AJ (1998) Automated docking using a Lamarckian genetic algorithm and an empirical binding free energy function. *J Comput Chem* 19:1639–1662
 37. Berendsen HJC, van der Spoel D, van Drunen R (1995) GROMACS: a message-passing parallel molecular dynamics implementation. *Comput Phys Commun* 91:43–56
 38. Lindahl E, Hess B, van der Spoel D (2001) GROMACS 3.0: a package for molecular simulations and trajectory analysis. *J Mol Model* 7:306–317
 39. Daura X, Mark AE, van Gunsteren WF (1998) Parameterization of aliphatic CH_n united atoms of GROMOS96 force field. *J Comput Chem* 19:535–547
 40. Schüttelkopf AW, van Aalten DMF (2004) PRODRG: a tool for high-throughput crystallography of protein-ligand complexes. *Acta Crystallogr D* 60:1355–1363
 41. Hess B, Bekker H, Berendsen HJC, Fraaije JGEM (1997) LINCS: a linear constraint solver for molecular simulation. *J Comput Chem* 18:1463–1472
 42. Berendsen HJC, Postma JPM, van Gunsteren WF, Dinola A, Haak JR (1984) Molecular dynamics with coupling to an external bath. *J Chem Phys* 81:3684–3690
 43. Darden T, York D, Pedersen L (1993) Particle mesh ewald: an N. log(N) method for ewald sums in large systems. *J Chem Phys* 98:10089–10092
 44. Patra M, Karttunen M, Hyvonen MT, Falck E, Lindqvist P, Vattulainen I (2003) Molecular dynamics simulations of lipid bilayers: major artifacts due to truncating electrostatic interaction. *Biophys J* 84:3636–3645
 45. Kabsch W, Sander C (1983) Dictionary of protein secondary structure: pattern recognition of hydrogen-bonded and geometrical features. *Biopolymers* 22:2577–2637
 46. Humphrey W, Dalke A, Schulten K (1996) VMD: visual molecular dynamics. *J Mol Graphics* 14:33–38
 47. Yang C, Li JY, Li Y, Zhu XL (2009) The effect of solvents on the conformations of Amyloid β -peptide (1–42) studied by molecular dynamics simulation. *THEOCHEM* 895:1–8
 48. Tjernberg LO, Tjernberg A, Bark N, Shi Y, Ruzsicska BP, Bu Z, Thyberg J, Callaway DJE (2002) Assembling amyloid fibrils from designed structures containing a significant amyloid β -peptide fragment. *Biochem J* 366:343–351
 49. Torok M, Milton S, Kaye R, Wu P, McIntire T, Glabe CG, Langen R (2002) Structure and dynamics features of Alzheimer's A β peptide in amyloid fibrils studied by site-directed spin labelling. *J Biol Chem* 277:40810–40815
 50. Balbach JJ, Petkova AT, Oyler NA, Antzutkin ON, Gordon DJ, Meredith SC, Tycko R (2002) Supramolecular structure in full-length Alzheimer's β -amyloid fibrils: evidence for a parallel β -sheet organization from solid-state nuclear magnetic resonance. *Biophys J* 83:1205–1216
 51. Shen L, Ji HF, Zhang HY (2008) Why is the C-terminus of A β (1–42) more unfolded than that of A β (1–40)? Clue from hydrophobic interaction. *J Phys Chem B* 112:3164–3167
 52. Tarus B, Straub JE, Thirumalai DJ (2006) Dynamics of Asp23-Lys28 salt-bridge formation in A β 10–35 monomers. *J Am Chem Soc* 128:16159–16168
 53. Lazo ND, Grant MA, Condron MC, Rigby AC, Teplow DB (2005) On the nucleation of amyloid β -protein monomer folding. *Protein Sci* 14:1581–1596

54. Sciarretta KL, Gordon DJ, Petkova AT, Tycko R, Meredith SC (2005) A β 40-lactam(D23/K28) models a conformation highly favorable for nucleation of amyloid. *Biochemistry* 44:6003–6014
55. Luhrs T, Ritter C, Adrian M, Riek-Loher D, Bohrmann B, Dobeli H, Schubert D, Riek R (2005) 3D structure of Alzheimer's amyloid- β (1–42) fibrils. *Proc Natl Acad Sci USA* 102:17342–17347
56. Knecht V, Mhwald H, Lipowsky R (2007) Conformational diversity of the fibrillogenic fusion peptide B18 in different environments from molecular dynamics simulations. *J Phys Chem B* 111:4161–4170